Validating the genetic alterations in cutaneous T-cell lymphoma: unraveling the role of SOCS1 and HNRNPK through genetically engineered mouse models

Luo, Y.

5

Role of *HNRNPK* Deletion in Initiating Cutaneous T-Cell Lymphoma Pathogenesis: An Inducible Knockout Mouse Model

Yixin Luo[1], Maarten H. Vermeer[1], Julia Van de Bie[1], Sanne de Haan[1], Peter Hohenstein[2], Frank R. de Gruijl[1], Cornelis P. Tensen[1]
1.Department of Dermatology, Leiden University Medical Center, Leiden, The Netherlands
2.Transgenic Facility Leiden, Central Animal Facility, Leiden University Medical Center, The Netherlands

The manuscript has been prepared and is ready for submission

Abstract:

Background: Recent genomic analysis has unveiled recurrent heterogeneous nuclear ribonucleoprotein K (*HNRNPK*) gene deletions in cutaneous T-cell lymphoma (CTCL). *HNRNPK* acts as a tumor suppressor by inhibiting the JAK-STAT pathway. **Objective**: This study investigates the pivotal role of *Hnrnpk* deletion in initiating CTCL pathogenesis using a transgenic mouse model. **Methods and Results**: *Hnrnpk* was knocked out in skin-infiltrating CD4+ T cells in transgenic mice (oxazolone, OXA, contact allergic reaction followed by topical tamoxifen to activate k.o.) which were then subjected to repeated applications of OXA (3-2/wk for 20 wks). After discontinuing OXA, autonomous inflammation persisted. Remarkably, *Hnrnpk* haploinsufficiency alone was sufficient to elicit these phenotypic changes. Comprehensive flow cytometry analyses of blood samples in the course of the experiment showed no evident effect but post mortem analyses of skin samples corroborated and characterized the persistent inflammation. Histological examinations revealed increased epidermal thickness and inflammatory cell infiltration, particularly CD3+ CD4+ T-cells, in *Hnrnpk* knockout mice exposed to long-term OXA treatment. Immunohistochemistry demonstrated heightened cell proliferation (Ki-67 expression) and augmented JAK-STAT signaling (p-STAT3) in these mice – all reminiscent of early CTCL. **Conclusion**: Our results underscore the significance of *Hnrnpk* deletion in CD4+ T-cells leading to autonomous skin inflammation, emulating early stages of CTCL, thereby confirming *HNRNPK*'s tumor-suppressive role. This *in vivo* model gives experimental access to the intricate processes involving *HNRNPK* in T-cell modulation, affecting epidermal homeostasis, and in CTCL pathogenesis, opening new avenues for potential therapeutic interventions.

Key words: Cutaneous T-cell lymphomas; JAK-STAT Pathway; CD4+ T cells; *HNRNPK*; Transgenic mouse

1 Introduction

Recent genomic analysis of cutaneous T-cell lymphoma (CTCL) has revealed recurrent deletion of the heterogeneous nuclear ribonucleoprotein K (*HNRNPK*) gene in two of the most common subtypes of CTCL, mycosis fungoides (MF) and Sézary syndrome (SS). (1-3) *HNRNPK* is a tumor suppressor gene that inhibits the JAK-STAT signaling pathway, and its deletion can lead to dysfunction of *HNRNPK*, which affects RNA processing and gene expression regulation. (4-6)

The potential impact of haploinsufficiency in this tumor suppressor gene is one of the notable characteristics of *HNRNPK*. *HNRNPK* haploinsufficiency resulted in reduced survival, increased tumor formation, genomic instability, and the development of transplantable hematopoietic neoplasms with myeloproliferation. (7) Haploinsufficiency of tumor suppressor genes (TSGs) can contribute to tumor development and progression by reducing levels of proteins, accelerating tumor development, promoting cancer progression, and collaborating with other haploinsufficient TSGs. (8-10)

The deletion of *HNRNPK* and other tumor suppressor genes (such as *SOCS1*, *STK11*, and *CDKN2A/B*) involved in commonly deregulated pathways in MF has been identified through next-generation sequencing (NGS) analysis. (1) A new mouse model with conditional *HNRNPK* knockout has been successfully established, which solves the lethality issue of direct *HNRNPK* knockout and confirms that this new mouse strain maintains relatively undisturbed immune homeostasis in the peripheral blood under chronic antigen exposure.

This study utilized a novel strain of homozygous and heterozygous mice to elucidate the role of *Hnrnpk* as an initiating factor when deleted in skin-homing CD4+ T cells, combined with repeated exposure to OXA simulation skin inflammation. Even after discontinuing 20 weeks of OXA applications, lymphocytic infiltration persisted, resulting in an authonomous inflammation with increased cell proliferation and sustained JAK-STAT pathway activation; features consistent with precursor stages of CTCL. A comparison between *Hnrnpk* double-copy deletion and *Hnrnpk* single-copy deletion mice revealed that the loss of a single allele of the *Hnrnpk* gene was already sufficient to cause this phenotypical change.

In sum, we investigated the role of *Hnrnpk* deletion as an initiating factor in the pathogenesis of CTCL in skin-homing CD4+ T cells, confirming the tumor-suppressive function of *Hnrnpk* and the impact of haploinsufficiency.

2.Result

2.1.Contact-allergic reaction in inducible *Hnrnpk* knock-out mice from long-term and

short-term oxazolone treatment groups

To determine the effect of oxazolone (OXA) treatment in inducing and maintaining inflamed skin in inducible *Hnrnpk* knock-out mice, a 1.5% concentration of OXA was administered topically on the shaved abdominal skin to sensitize *Hnrnpk fl/fl Cd4CreER^{T2}*+/- (FL/FL), *Hnrnpk fl/wt Cd4CreER^{T2}*+/- (FL/WT), and *Hnrnpk wt/wt Cd4CreER^{T2}*+/- (WT/WT) mice. Subsequently, a 0.5% concentration of OXA was applied 3 times a week (initially, and then twice after 10 weeks) on the shaved left flank from week 2 to week 20 (**Figure 1A**). This regimen established the experimental group as the long-term OXA group. An additional group of mice was included as a control group for the initial short-term OXA exposure. This group did not receive any application of 0.5% OXA on their skin from week 2 to week 20, as depicted in **Figure 1B.**

In both experimental groups, none of the mice displayed any signs of wounding from scratching in response to a possible pruritus (**Supplementary Figures 1 and 2**). Visible signs of inflammation, such as redness, flaking, and a rough texture, were observed on the treated flanks of all mice one day after the first application of 0.5% OXA on the skin. In contrast, the untreated skins of all mice in both long-term and short-term OXA treatment groups did not show any indication of inflammation.

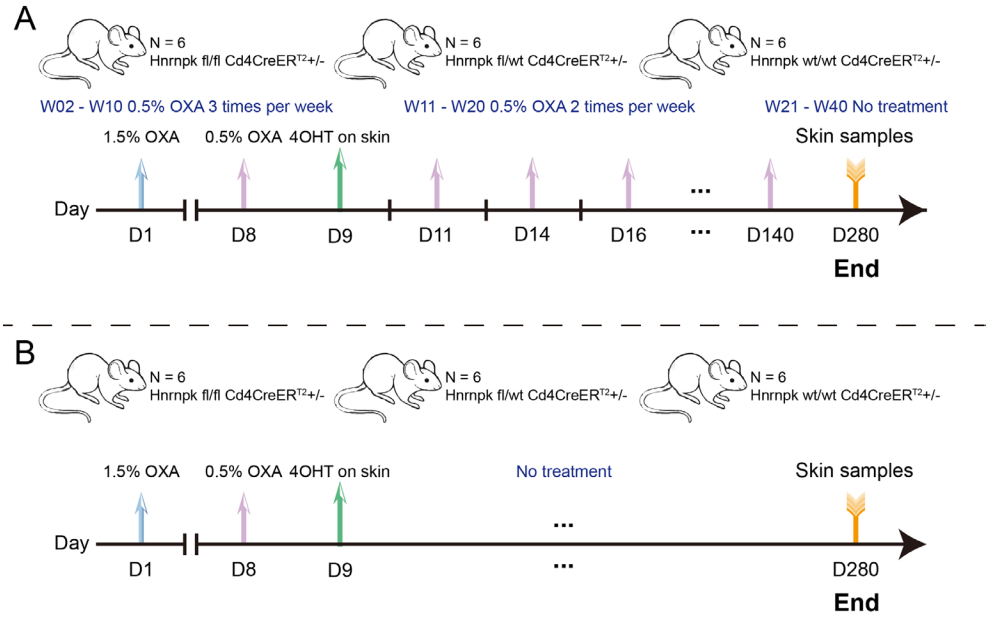

Figure 1. Schematic time-course representation of the experimental groups and different treatment

periods with oxazolone. (A). Long-term treatment period: the left flanks of *Hnrnpk fl/fl Cd4CreER^{T2}*+/-, *Hnrnpk fl/wt Cd4CreER^{T2}*+/- and *Hnrnpk wt/wt Cd4CreER^{T2}*+/- mice were treated with OXA 3 times per week from week 2 to 10 and 2 times per week from week 11 to 20. From week 21 to 40, no OXA was administrated on the skin of the mice. B) Short-term treatment period: *Hnrnpk fl/fl Cd4CreER^{T2}*+/-, *Hnrnpk fl/wt Cd4CreER^{T2}*+/- and *Hnrnpk wt/wt Cd4CreER^{T2}*+/- mice without OXA treatment from week 2 to 40. In both treatment groups the mice were treated on day 1 and 8 with OXA and 4OHT was applied on day 9. Mice were sacrificed on day 280. n is 6 per genotype. Abbreviations: D is day, W is week, OXA is oxazolone, 4OHT is 4-hydroxy-tamoxifen. Blood collection was performed 24 hours after OXA application. Skin samples were collected at the end of the experiment.

2.2.Long-term oxazolone application caused local skin inflammation rather than systemic effect

Flow cytometry analysis showed successful cell extraction post mortem from mouse skin, and the proportion of CD4+ and CD8+ cells among CD3+ cells was determined. (**Figure 2A**) The long-term OXA group exhibited a statistically significant increase in the proportion of CD4+ cells among CD3+ cells in the treated flanks of *Hnrnpk* knockout mice (FL/FL and FL/WT), as compared to the treated flanks of WT/WT mice. No statistically significant disparity is observed in the proportion of CD4+ cells among CD3+ cells in the treated flanks when comparing FL/FL and FL/WT conditions. (**Figure 2B**) In addition, there was a notable rise in the proportion of CD4+ cells to CD3+ cells in the treated flanks of *Hnrnpk* knockout mice (FL/FL and FL/WT) compared to the untreated flanks. Similar results were seen for the fraction of CD8+ cells among CD3+ cells. (**Figure 2C**) In the short-term OXA treatment group, no statistically significant differences were observed between the treated and untreated flanks when comparing across all groups.

Flow cytometry analysis was performed on the peripheral blood samples collected weekly from the mice in both experimental groups. The ratio of circulating CD3+ and CD19+ cells and CD4+ and CD8+ cells was measured to assess the overall status of the mice's immune system. In both the long-term and short-term groups, the peripheral blood of all mice did not show any disturbance in the ratio of CD3+ cells to CD19+ cells. (**Figure 2D**) Likewise, the proportion of CD4+ cells to CD8+ cells in the peripheral blood of all mice exhibited no noticeable variations. (**Figure 2E**) Throughout the investigation, the sub-population ratios of immune cells remained relatively stable.

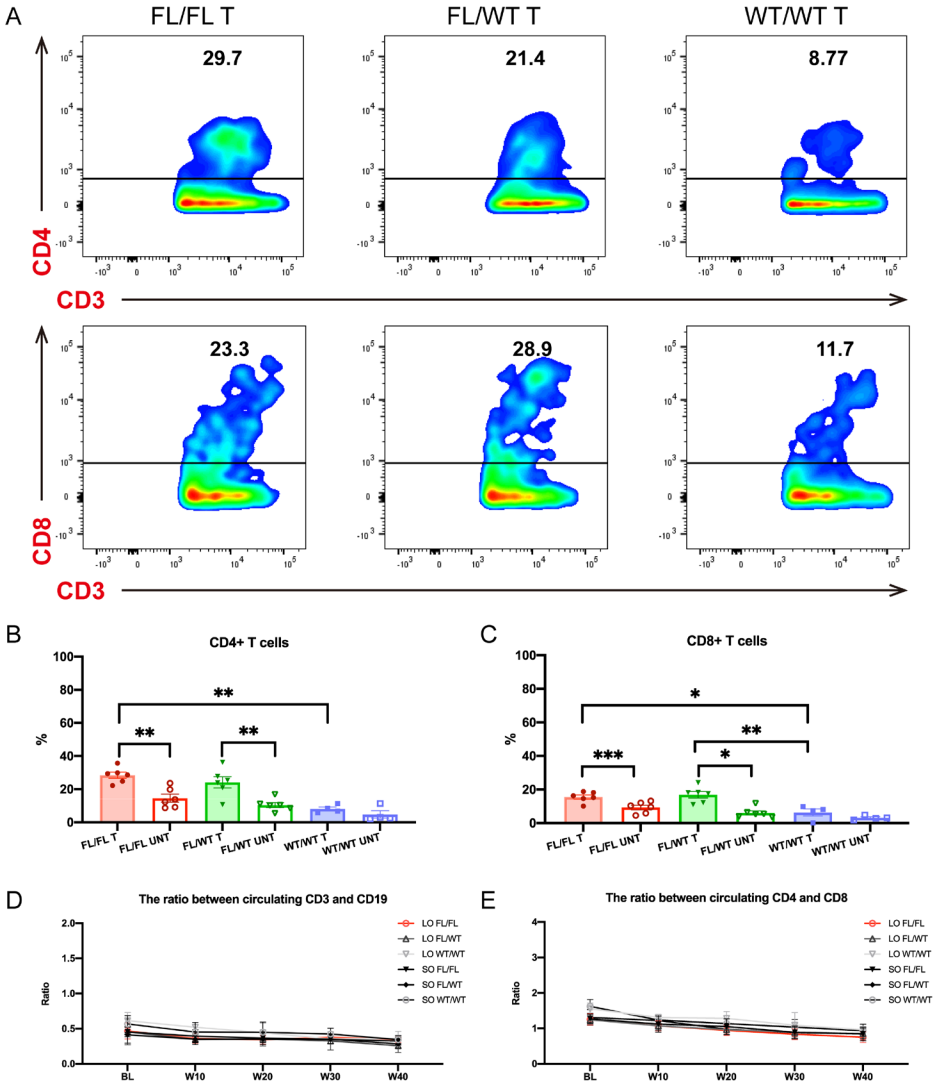

Figure 2. Flow cytometry analysis of skin and peripheral blood of *Hnrnpk fl/fl Cd4CreER*^{T2}+/-, *Hnrnpk fl/wt Cd4CreER*^{T2}+/- and *Hnrnpk wt/wt Cd4CreER*^{T2}+/- mice from the long-term and short-term OXA treatment groups showed T cells infiltration in skin and no systemic inflammation. (A). Representative flow cytometry plots and quantitative analysis of CD3+ CD4+ T cells and CD3+ CD8+ T cells in treated flanks of mice from the long-term group. (B) The quantitative analysis of CD3+ CD4+ T cells in the flanks of mice from long-term group. (C) The quantitative analysis of CD3+ CD8+ T cells in the flanks of mice from long-term group. (D) The ratio of CD3 to CD19 cells isolated from peripheral blood of mice in both long-term and short-term groups. (E) The ratio of CD4 to CD8 cells isolated from peripheral blood of mice in both long-term and short-term groups. Abbreviations: FL/FL is *Hnrnpk*

fl/fl Cd4CreER^{T2}+/-. FL/WT is *Hnrnpk fl/wt Cd4CreER*^{T2}+/-. WT/WT is *Hnrnpk wt/wt Cd4CreER*^{T2}+/-. T is treated flank. UNT is untreated flank. 'LO' is the long-term OXA treatment group, and 'SO' is the short-term OXA treatment group.

2.3.*Hnrnpk* deletion with long-term oxazolone treatment caused autonomous skin inflammation

HE staining was conducted on skin samples to assess and quantify the number of epidermal layers in the long-term and short-term treatment groups (**Figure 3, & Supplementary Figure 3**). In the long-term OXA group, the number of epidermal layers in treated flanks from FL/FL and FL/WT mice were significantly greater than those in untreated sides (**Figures 3A, & 3B**). There were no significant differences between genotypes. In the short-term treatment group, there were no statistically significant differences in the number of epidermal layers between the FL/FL and FL/WT mice and the WT/WT mice and the treated and untreated flanks from the same genotype. This showed that *Hnrnpk* deletion, in combination with long-term OXA treatment, caused a significant inflammatory response.

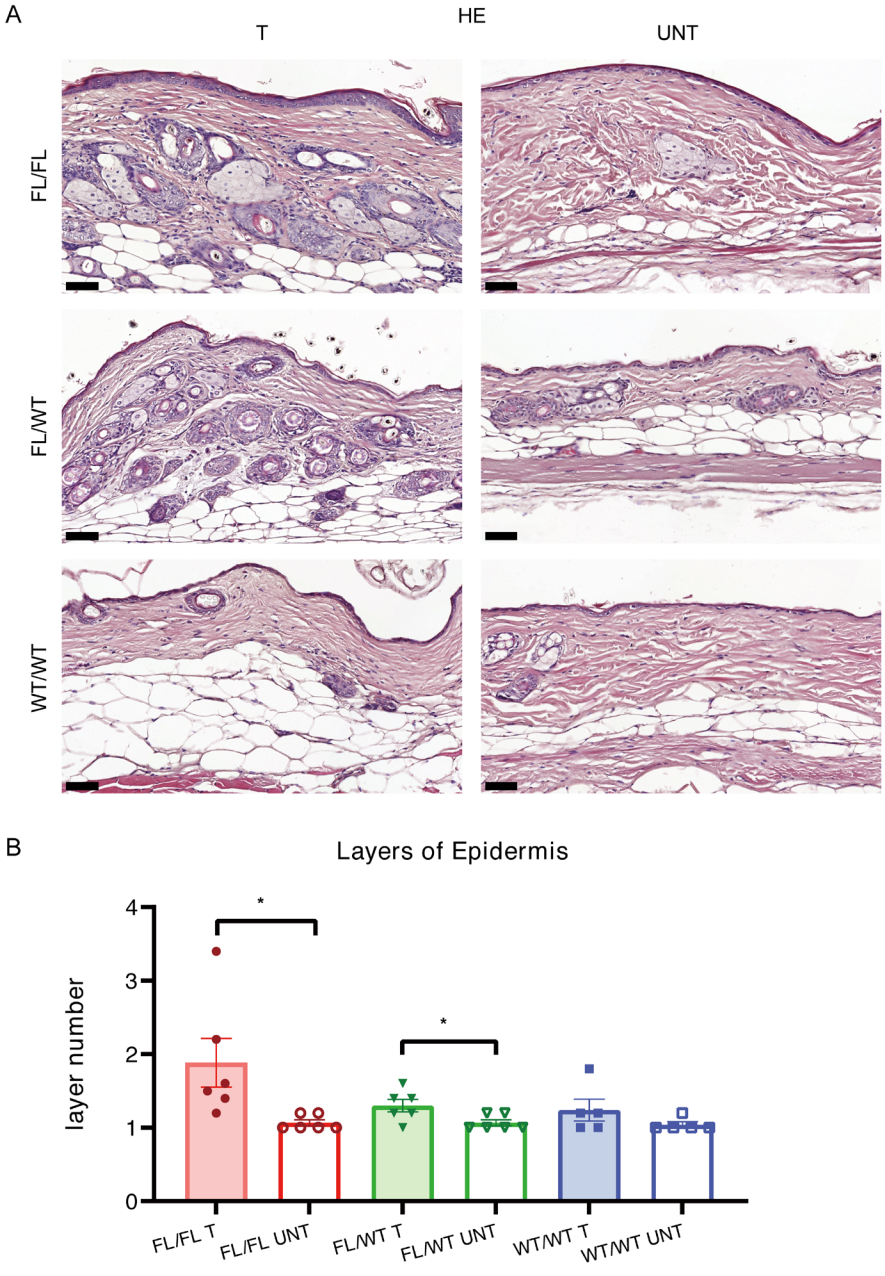

Figure 3. Histological examination of skin sections from the long-term treatment group indicated an increased number of epidermal layers in the treated flanks of *Hnrnpk fl/fl Cd4CreER*^{T2}+/- and *Hnrnpk fl/wt Cd4CreER*^{T2}+/- mice. (A). HE stained sections from treated and untreated flanks of mice in the long-term treatment group. Magnification is 20x and scale bar is 50 µm. (B) Quantification of the

number of epidermal layers of treated and untreated skin of the mice from long-term treatment group. Paired t-test and two-way ANOVA with a Tukey's post hoc test were used for statistical analysis. Error bars represent SEM and * indicates a significant difference (*$P < 0.05$). n is 5 or 6 per genotype. Abbreviations: FL/FL is *Hnrnpk fl/fl Cd4CreER^{T2}*+/-. FL/WT is *Hnrnpk fl/wt Cd4CreER^{T2}*+/-. WT/WT is *Hnrnpk wt/wt Cd4CreER^{T2}*+/-. T is treated flank. UNT is untreated flank.

2.4.*Hnrnpk* deletion increased the number of lymphocytes and caused autonomous skin inflammation

To evaluate the inflammatory response in the skin of transgenic mice, IHC staining was conducted to quantify the amount of CD3+, CD4+, and CD8+ T-cells in the dermis of the long-term and short-term OXA groups (**Figure 4; Supplemental Figures 4, 5 & 6**). The number of CD3+ and CD4+ positive stained cells in the treated flanks of transgenic mice (FL/FL and FL/WT) was considerably and statistically significantly higher in the long-term OXA group compared to the treated flanks of WT/WT mice (**Figure 4A, 4B, & 4C**). Moreover, the number of CD3+ and CD4+ cells in the dermis of the treated flanks of FL/FL and FL/WT mice was statistically significantly higher than in the untreated flanks (**Figures 4A, 4B, & 4C; Supplemental Figure 5**). Similar observations were made for CD8+ positive stained cells (**Figures 4A, & 4D; Supplemental Figure 5**). However, no significant change was seen between the treated flank sections of FL/FL mice and FL/WT mice. CD3+, CD4+, and CD8+ T-cells in the long-term OXA group showed in clusters. The short-term OXA group had no significant increases in inflammatory cells within or between groups. (**Supplementary Figures 4, & 6**). In untreated flanks, these findings showed that CD3+, CD4+, and CD8+ T-cells were more abundant in the treated skin sections of the transgenic mice in the long-term OXA group, particularly in the FL/FL and FL/WT mice when compared to the WT/WT mice, clearly showing that *Hnrnpk* loss along with long-term OXA treatment increased the skin inflammatory response.

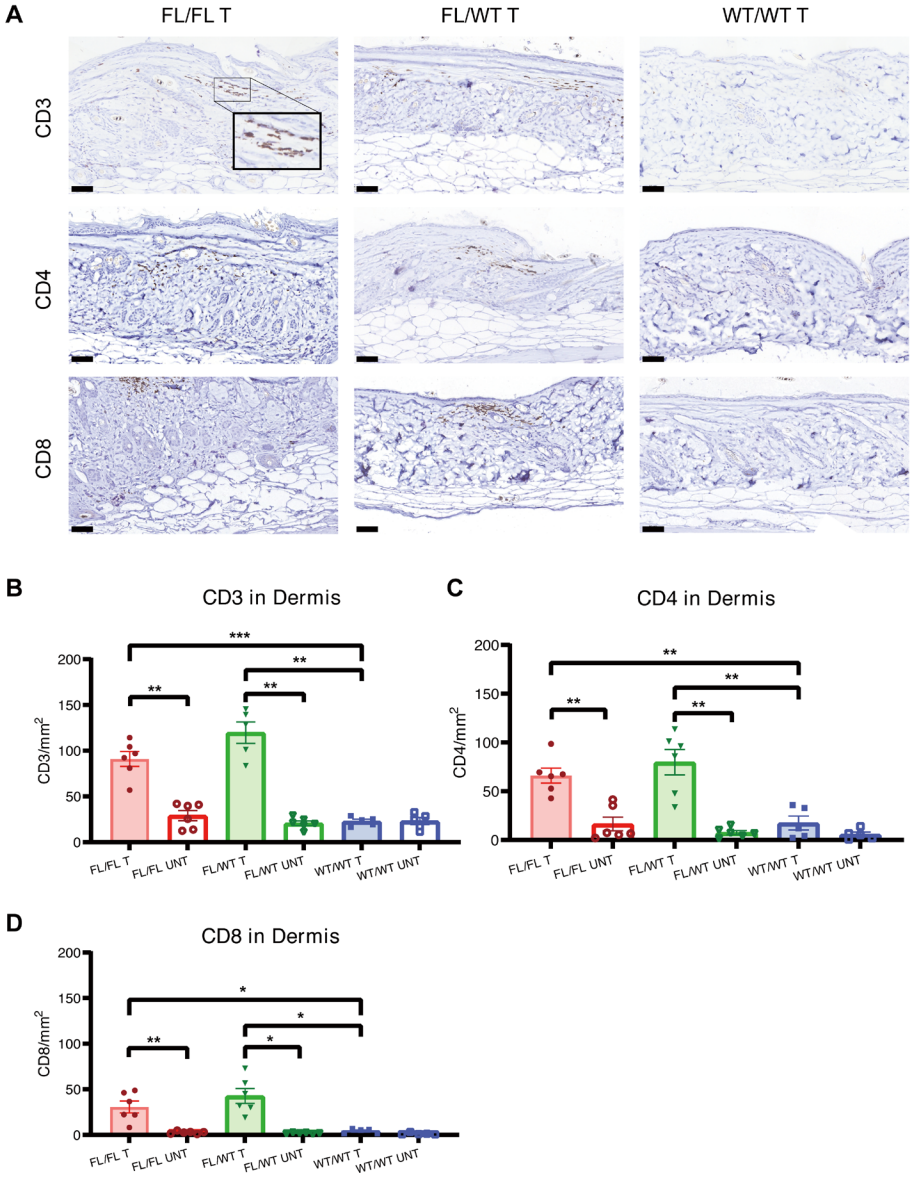

Figure 4. Histological analysis of treated skins from *Hnrnpk fl/fl Cd4CreER*^{T2}+/-, *Hnrnpk fl/wt Cd4CreER*^{T2}+/- and *Hnrnpk wt/wt Cd4CreER*^{T2}+/- mice of the long-term treatment group revealed increased number of CD3+, CD4+ and CD8+ cells in dermis. (A). Skin sections from the treated flanks of mice in the long-term treatment group, stained with markers for CD3, CD4, and CD8. Magnification is 20x and scale bar is 50 µm. (B, C, D) Quantification of the positive stained CD3+ (B), CD4+ (C) and CD8+ (D) cells in the dermis of treated (T) and untreated (UNT) flanks of the mice in

long-term treatment group. Paired *t*-test and two-way ANOVA with a Tukey's post hoc test were used for statistical analysis. Error bars represent SEM and * indicates a significant difference (*$P < 0.05$, **$P < 0.01$, ***$P < 0.001$, ****$P < 0.0001$). n is 5 or 6 per genotype. Abbreviations: FL/FL is *Hnrnpk fl/fl Cd4CreER^{T2}+/-*. FL/WT is *Hnrnpk fl/wt Cd4CreER^{T2}+/-*. WT/WT is *Hnrnpk wt/wt Cd4CreER^{T2}+/-*. T is treated flank. UNT is untreated flank.

2.5.Loss *Hnrnpk* in autonomous skin inflammation affected cell proliferation index

To investigate the impact of *Hnrnpk* deletion in CD4+ T-cells Ki-67 immunohistochemical staining was conducted on dermal samples of both the long-term and short-term treatment groups. The results of this analysis are presented in **Figure 5** and Supplementary **Figure 7**. The long-term treatment group exhibited a notable increase in Ki-67 positive cells in the flanks of FL/FL and FL/WT mice compared to WT/WT mice (**Figure 5A, & 5B**). Furthermore, a notable increase in Ki-67 activation was observed in both the dermis of the treated compared to those untreated flanks in FL/FL and FL/WT groups (**Figure 5A, & 5B**). No significant changes were found within and between the genotypes in the short-term therapy group (**Supplemental Figure 7**). The results of this study indicated that the levels of Ki-67 cells were enhanced in the treated skin sections of the transgenic mice subjected to to the long-term treatment. This showed that combining *Hnrnpk* deletion and long-term OXA treatment increased cell proliferation.

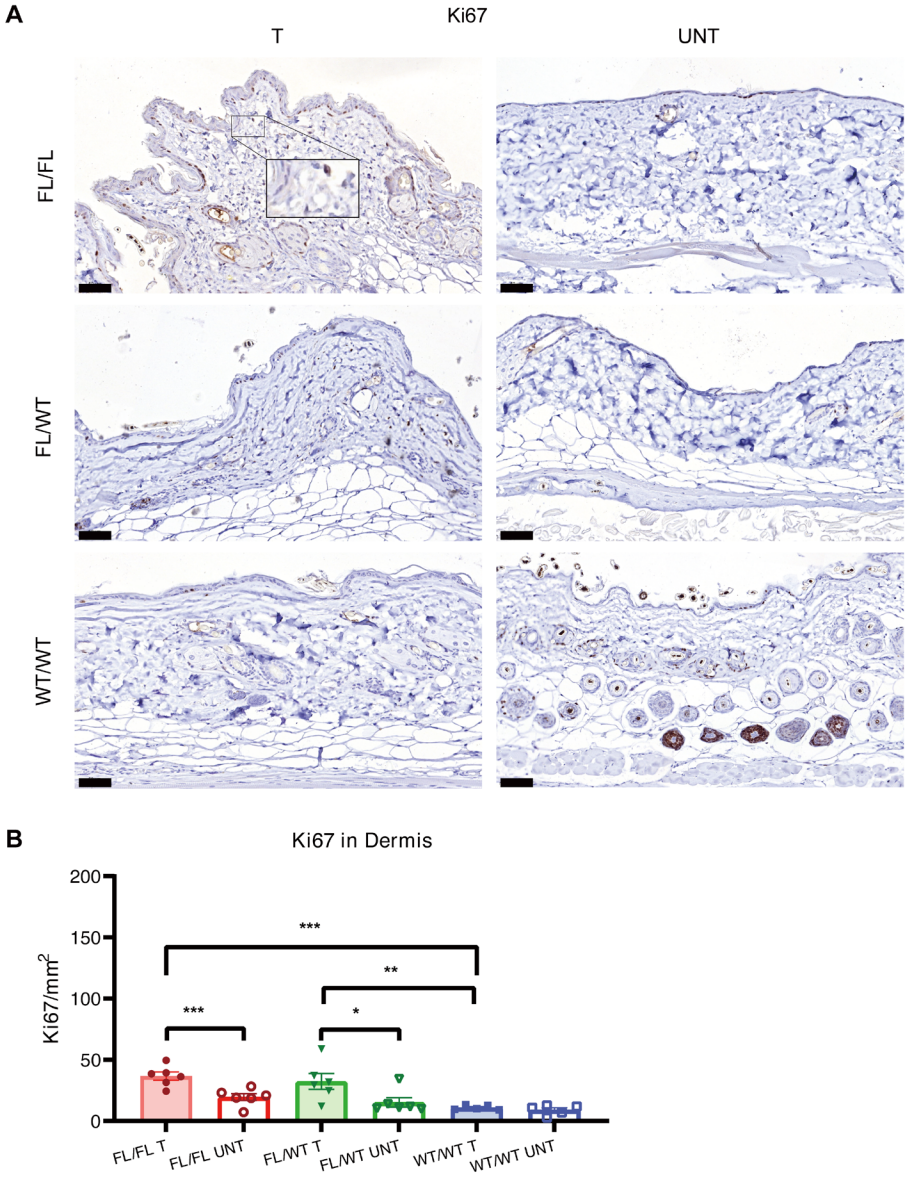

Figure 5. Histological analysis of treated and untreated skins from *Hnrnpk fl/fl Cd4CreER*^{T2}+/-, *Hnrnpk fl/wt Cd4CreER*^{T2}+/- and *Hnrnpk wt/wt Cd4CreER*^{T2}+/- mice of the long-term treatment group revealed increased number of Ki-67 positive cells in dermis. (A). Skin sections from the treated and untreated flanks of mice in the long-term treatment group, stained with Ki67. Magnification is 20x and scale bar is 50 µm. (B). Quantification of the positive stained p-STAT3 cells in dermis of treated and untreated skins of the mice from long-term treatment group. Paired *t*-test and two-way ANOVA with a Tukey's post hoc test were used for statistical analysis. Error bars represent SEM and *

indicates a significant difference (*$P < 0.05$, ***$P < 0.001$, ****$P < 0.0001$). n is 5 or 6 per genotype. Abbreviations: FL/FL is *Hnrnpk fl/fl Cd4CreER^{T2}+/-*. FL/WT is *Hnrnpk fl/wt Cd4CreER^{T2}+/-*. WT/WT is *Hnrnpk wt/wt Cd4CreER^{T2}+/-*. T is treated flank. UNT is untreated flank.

2.6.Loss *Hnrnpk* in autonomous skin inflammation affected the JAK-STAT signaling pathway

IHC staining was performed to analyze the number of p-STAT3 positive cells in the dermis of the long-term and short-term treatment groups to see if the *Hnrnpk* deletion in CD4+ T-cells with persistent skin inflammation affected the JAK-STAT signaling pathway (**Figure 6; Supplementary Figure 8**). In the long-term OXA group, the treated flanks of FL/FL and FL/WT mice had a significantly higher number of p-STAT3 positive cells than those of WT/WT mice (**Figures 6A, & 6B**). Furthermore, p-STAT3 activation was significantly higher in the treated flanks' dermis than in the untreated flanks of FL/FL and FL/WT mice (**Figures 6A**, **& 6B**). There were no significant changes among or between genotypes in the short-term OXA group (**Supplementary Figures 8**). These data revealed that p-STAT3 cells were more numerous in the treated flanks of transgenic mice in the long-term OXA group, implying that *Hnrnpk* deletion combined with long-term OXA boosted Stat3 activation, enhancing the JAK-STAT signaling pathway.

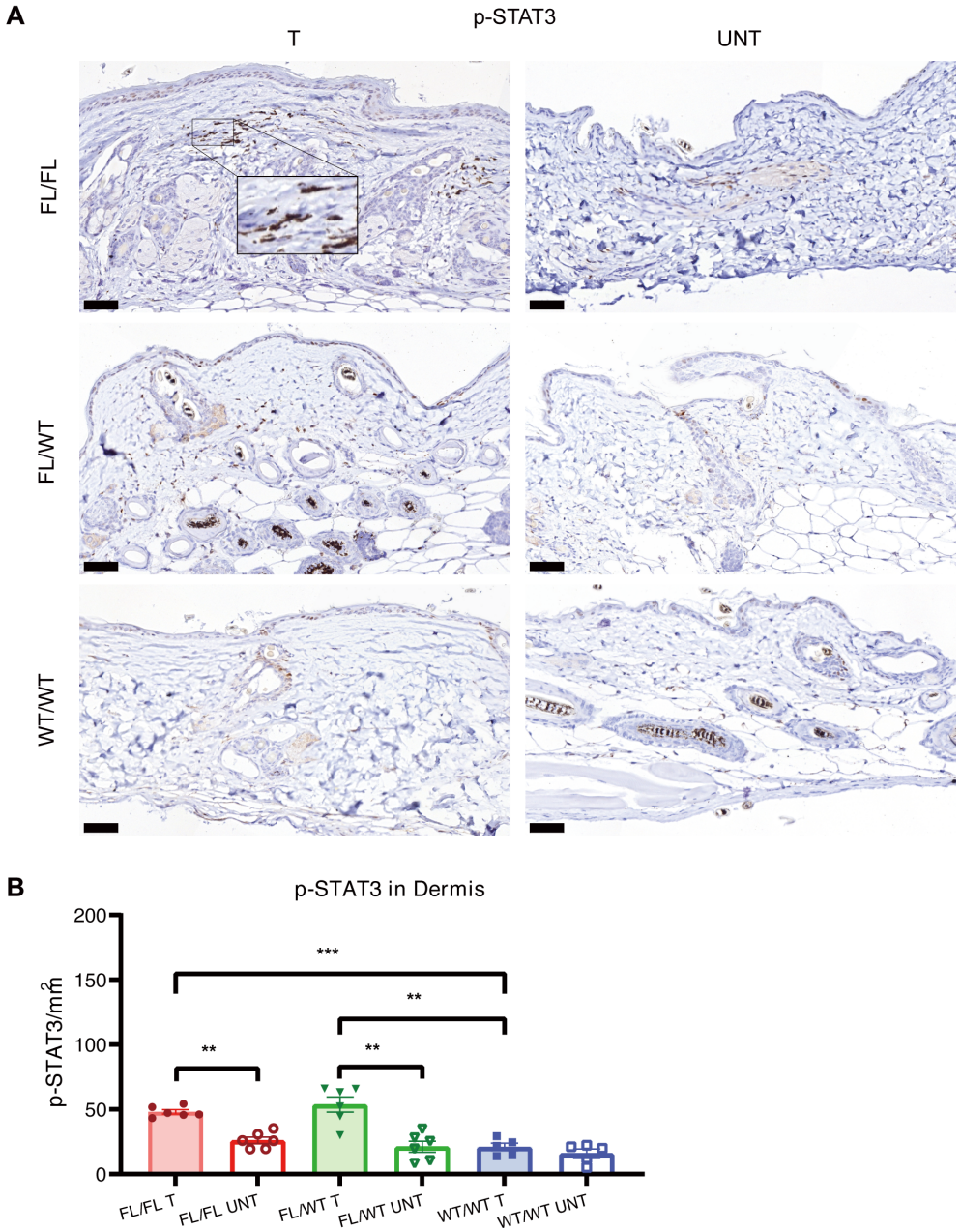

Figure 6. Histological analysis of treated and untreated skins of *Hnrnpk fl/fl Cd4CreER*^{T2}+/-, *Hnrnpk fl/wt Cd4CreER*^{T2}+/- and *Hnrnpk wt/wt Cd4CreER*^{T2}+/- mice from the long-term treatment group revealed increased number of p-STAT3 positive cells in dermis. (A). Skin sections from the treated and untreated flanks of mice in the long-term treatment group, stained with p-STAT3. Magnification is 20x and scale bar is 50 µm. (B). Quantification of the positive stained p-STAT3 cells in dermis of treated and untreated flanks of mice from the long-term treatment group. Paired *t*-test and two-way

ANOVA with a Tukey's post hoc test were used for statistical analysis. Error bars represent SEM and * indicates a significant difference (*$P < 0.05$, ***$P < 0.001$, ****$P < 0.0001$). n is 5 or 6 per genotype. Abbreviations: FL/FL is *Hnrnpk fl/fl Cd4CreER^{T2}*+/-. FL/WT is *Hnrnpk fl/wt Cd4CreER^{T2}*+/-. WT/WT is *Hnrnpk wt/wt Cd4CreER^{T2}*+/-. T is treated flank. UNT is untreated flank.

3.Discussion

This study showed that transgenic mice with *Hnrnpk* deletion in CD4 skin-infiltrating cells and subsequent repeated OXA applications resulted in features of early-stage cutaneous T cell lymphoma. These included autonomous skin inflammation, CD3+ CD4+ lymphocytic infiltration, increased Stat3 signaling, and enhanced lymphocyte proliferation index. Our findings supported prior studies by demonstrating the CTCL-like features associated with both biallelic and monoallelic *Hnrnpk* deletions, shedding light on their significant impact and likely underlying pathways in CTCL formation.

Our previous experience with OXA application revealed that applying modest doses to the skin surface three times a week could reduce skin inflammation without any discomfort. (11) Nevertheless, in the present study, we observed an increase in epidermal layer thickness and dermal infiltration by inflammatory cells in the treated flanks of Hnrnpk knockout mice in the long-term OXA group.

While previous research has indicated *HNRNPK*'s involvement in regulating T-cell activation and cytokine production, the precise role of *HNRNPK* in influencing the infiltration of inflammatory cells in the dermis remains inconclusive. (12) This study added to the body of evidence by revealing the various impacts of *HNRNPK* on T-cell activity.

An earlier research has shown that reduced *Hnrnpk* expression in mice resulted in the development of malignant T-cell lymphoma, marked by the expansion of abnormal lymphocytes and an increase in pro-inflammatory cytokines such as IL-2 and TNF-a. (7) The dual role of *HNRNPK* in tumor suppression and inflammation promotion is also evident in acute myeloid leukemia and lung cancer. (13, 14) Given the inconsistent results of earlier investigations, the mechanisms by which *HNRNPK* deficiency increases inflammation and cancer remain unknown. Some studies have even proposed that *HNRNPK* acts as an oncogene due to its elevated levels in various inflammation-related malignancies, including melanoma, colorectal, and prostate cancer. (15-17) These divergent findings underscore the importance of maintaining the homeostatic balance of *HNRNPK* expression in preventing disease mechanisms and tumor formation. Our study further supports *HNRNPK* deletion increased cell proliferation (Ki-67 expression) and JAK-STAT pathway activation.

In the context of cancer, *HNRNPK* has been suggested to have a dual role, acting as both a

tumor suppressor and an oncogene. (7) A role as oncogene is supported by the notion that elevated *HNRNPK* expression is associated with increased Ki-67 expression in breast cancer (18), down-regulation led to impaired proliferation in head and neck squamous carcinoma with reduced Ki-67 expression. Overexpression of *HNRNPK* in a mouse model increased tumor size and Ki-67 expression, while *HNRNPK* knockdown reduced tumor size and Ki-67 expression. (19). For AML and CTCL a tumor suppressor function for *HNRNPK* is more likely. Our mouse model shows that the proliferation marker Ki-67, which increases with disease progression and has been identified as a prognostic marker in MF, particularly in tumor-stage (20, 21) is increased after knockout of *Hnrnpk* in CD4+ T cells. (22, 23)

The JAK-STAT3 signaling pathway has been confirmed to play a significant role in CTCL pathogenesis. Persistent activation of STAT3 has been observed in CTCL and identified as a driving force behind this malignant condition. (24) Aberrantly active STAT3 promotes tumor cell survival, proliferation, upregulation of immune suppressive factors, and inhibition of Th1 mediators, among other oncogenic properties. (25) Constitutive activation of STAT3 is associated with malignant T-cell proliferation, resistance to apoptosis, and inflammation in CTCL. The expression of phosphorylated STAT3 and its critical role in the survival of CTCL cell lines have been documented. (26) Moreover, STAT3 is expressed in early-stage CTCL but not elevated in healthy skin dermis. (27) Sustained activation of Stat3 in T cells drives disease progression in a CTCL mouse model, although this model exhibited changes in STAT3 in all T cells rather than specifically in CD4+ T cells. (28) *HNRNPK* also inhibits cancer cell proliferation through the p53 signaling pathway, with p53, p21, and CCND1 playing pivotal roles. *HNRNPK*'s involvement in regulating the cancer proteome, including the STAT signaling pathway, also reinforces its influence on tumor growth. (29) (30) We observed enhanced JAK-STAT signaling in heterozygous and homozygous *Hnrnpk* knockout mice. These findings align with previous research suggesting lymphoma development is mediated through *Hnrnpk*-mediated Stat3 activation. (7)

Deletion of a single allele of the *Hnrnpk* gene is sufficient to influence the phenotype of the mouse model, with no significant differences observed between the phenotypes resulting from biallelic and monoallelic gene deletions. Our study included homozygous *Hnrnpk* knockout, heterozygous *Hnrnpk* knockout, and wild-type *Hnrnpk* mice, facilitating comprehensive genotype comparisons to enhance our understanding of the gene's function and its impact on the biological processes studied. (31) All experimental mice were subjected to identical environmental conditions, mitigating potential confounding factors and enhancing the reliability of the results. Considering the possible variability, the incorporation of various genotypes and the increase in the number of mice were crucial for obtaining more reliable and reproducible results. (32)

In conclusion, this extensive research underscores the pivotal role of *Hnrnpk* in CD4+ skin-homing T cells within chronically inflamed skin, exacerbating skin inflammation reminiscent of the early stages of MF. These findings suggest that *HNRNPK* may play an initiating role in the development of MF.

4.Methods and Materials

4.1.Mice

All mouse experiments were supervised by the animal welfare committee (IvD) of the Leiden University Medical Center and approved by the national central committee of animal experiments (CCD) under the permit number AVD116002015271, in accordance with the Dutch Act on Animal Experimentation and EU Directive 2020/63/EU.

Hnrnpk flox (*Hnrnpkem1*Lumc; MGI:99894) mice where loxP sites were introduced in *Hnrnpk* intron 2 and intron 6 were generated at LUMC. *Hnrnpk* flox mice using CrisprCas9 RNP and 200 bp single-stranded oligodeoxynucleotides (ssODN). *Cd4CreER^{T2}* mice (Tg (*Cd4-cre/ER^{T2}*)11Gnri/J; MGI:5493114; JAX:022356) expressing *CreER^{T2}* recombinase under the control of the *Cd4* promoter were purchased from The Jackson Laboratory (JAX). *Hnrnpk* flox mice were mated with *Cd4CreER^{T2}* mice to generate *Hnrnpk flox Cd4CreER^{T2}* mice. The offspring inherited both the targeted *Hnrnpk* flox allele and the *Cre* transgene.

Inducible homozygous (FL/FL) and heterozygous (WT/FL) *Hnrnpk* knockout mice were obtained by crossing conditional *Hnrnpk* knock-out mice (LUMC) with 4OHT inducible *Cd4-CreER^{T2}*-knock-in mice (Jackson's Laboratories) in the C57BL6/6J background. Resulted offspring was characterized by exon 3 to exon 6 deletion in *Hnrnpk* in *Cre*-expressing CD4+ T cells upon 4OHT administration. Wild type littermates (WT/WT) with *Cd4CreER^{T2}* in the C57BL6/6J background were used as a control group throughout the experiment. All mice were assigned to experimental or control groups based on their genotype. Treatments were assigned randomly. Mice were housed in a temperature-controlled room with a 12-hour light-dark cycle. Throughout the experiment, food and tap water were available ad libitum.

4.2.Oxazolone preparation and administration

Sensitization and inflammation of mouse skins were described as before.(33) The skin inflammation was induced by oxazolone (4-Ethoxymethylene-2-phenyl-2-oxazolin-5-one, OXA, Sigma-Aldrich) dissolved in acetone (Macron) to a concentration of 1.5% or 0.5% for each experiment. 1.5% OXA was used to sensitize shaved abdomen skins. After 1 week, 0.5% OXA was applied on shaved left flanks to induce skin inflammation. To maintain skin

inflammation, 0.5% OXA was administrated on shaved left flanks. As control, acetone was administrated on right shaved flanks. Before shaving and OXA treatment, mice were placed in isoflurane box and anesthetized with 2 - 4% isoflurane (Karizoo). Anesthesia was put on 0.25 - 2% isoflurane during shaving and OXA application.

4.3.4-hydroxy-tamoxifen preparation and administration

Cre-mediated deletion of *Hnrnpk* was performed in 6 to 20 weeks old mice with 4OHT (Sigma-Aldrich). 4OHT was dissolved in ethanol (J. T. Baker) and peanut oil (Sigma-Aldrich) to a concentration of 20 mg/ml. Dissolved 4OHT was placed in ultrasound sonicator (Branson 2510) for 2 minutes at room temperature and stored at 4 °C. Before each experiment, 4OHT was warmed to room temperature and administrated once on left shaved skins with 1 mg per mouse. As control, ethanol was administrated on right shaved flanks.

4.4.Flow cytometry

Skin cells were isolated by taking a 4 mm^2 skin biopsy post mortem, which was then digested using the whole skin dissociation Kit (Miltenyi Biotec, NL) following the manufacturer's instructions. Blood samples of mice (50 µL) were obtained from tail vein every week 24 hours after OXA treatment. Samples were transferred to tubes with lysis buffer (Hospital Pharmacy LUMC) and incubated for 10 minutes at 37 °C. After incubation, phosphate-buffered saline (PBS; Orphi Farma) was added to tubes and centrifuged for 5 minutes at 1600 rpm at room temperature. Lysates were transferred to FACS plates and centrifuged for 3 minutes at 1400 rpm at room temperature. Plates were washed with FACS buffer (Thermo Fisher Scientific). Fluorescence-labeled antibodies, anti-mouse CD3 (clone 145-2C11, BD Biosciences), anti-mouse CD19 (clone 1D3, Thermo Fisher Scientific), anti-mouse CD4 (clone RM4-5, Thermo Fisher Scientific) and anti-mouse CD8 (clone 53-6.7, Biolegend), were added to the cells and incubated for 30 minutes on ice. After incubation, cells were washed 2 times with FACS buffer and transferred to tubes with paraformaldehyde (PFA, Sigma-Aldrich). BD Fortessa flow cytometer was used for measurements and samples were analyzed with FlowJo software. For compensation, labeled beads (Thermo Fisher Scientific) were made by the same procedure and used shortly before the measurements.

4.5.Histological and immunohistochemical staining

Mice skin samples were obtained after CO2-mediated sacrifice and fixed with 4% PFA (Added Pharma). Skin tissues were dehydrated with increasing grade of ethanol (50%, 70%, 100%), cleared in xylene (J.T. Baker) and embedded in paraffin (Klinipath) using

Leica HistoCore Arcadia H machine. Embedded skins were placed in microtome (Leica 149MULTI0C1) and sliced at thickness of 4 µm. Skin sections were dewaxed with xylene and rehydrated with decreasing grade of ethanol (100%, 70%, 50%). Slides were stained with haematoxylin and eosin (HE) staining and dehydrated with increasing grade of ethanol (95% and 100%) followed by xylene. Skin sections were mounted on glass lids using Depex (Sigma-Aldrich).

For immunohistochemical (IHC) stainings, paraffin-embedded skin sections were dewaxed with xylene and rehydrated in 100% ethanol. Afterwards, skin sections were blocked with 0.3% hydrogen peroxidase (H202, Sigma-Aldrich) and rehydrated with decreasing grade of ethanol (95%, 85%, 70%). Antigen retrieval was performed in 0.01M sodium citrate solution (Merck; pH 6) for 10 minutes at low-medium in the microwave (Etna). Skin slices were washed 3 times with PBS/0.05% Tween (Sigma-Aldrich). Sections were blocked with SuperBlock (Thermo Fisher Scientific) for 30 minutes at room temperature and incubated with primary antibodies, anti-mouse CD3 (D7A6E, Cell Signaling Technology, dilution 1:200), anti-mouse CD4 (D7D2Z, Cell Signaling Technology, dilution 1:100), anti-mouse CD8 (4SM15, eBioscienceTM, dilution 1:1600) and anti-mouse p-STAT3 (D3A7, Cell Signaling Technology, dilution 1:150), at 4 °C overnight. All primary antibodies were dissolved in PBS with 1% bovine serum albumin (BSA, Thermo Fischer Scientific).

Next day, skin slices were washed 3 times with PBS/0.05% Tween and incubated with secondary antibody goat-anti-rabbit (IgG biotinylated, Sigma-Aldrich, dilution 1:200) or rabbit-anti-rat (IgG biotinylated, Sigma-Aldrich, dilution 1:200) dissolved in PBS/1% BSA for 30 minutes at room temperature. Sections were washed 3 times with PBS/0.05% Tween. Slides were incubated with Vectastain Elite Kit (Vector Labs, dilution 1:200) for 30 minutes at room temperature and washed 3 times with PBS. Skin sections were visualized with diaminobenzidine (DAB, Dako Omnis, dilution 1:100) for 5 minutes at room temperature and washed with MilliQ water. Nuclei were counterstained with filtered haematoxylin (dilution 1:5) for 3 seconds at room temperature. Skin slides were washed in tap and MilliQ water and dehydrated with increasing grade of ethanol (70%, 85%, 95%, 100%). Skin sections were mounted on glass lids using Entellan (Sigma-aldrich).

All slices were photographed and examined with bright field microscope scanner (3D HISTECH, Pannoramic 250). For HE analysis, epidermal layers of each skin section were counted at 20x magnification. Means were estimated and used for statistical analysis. For IHC analysis, CD3, CD4, CD8, Ki-67 and p-STAT3 positive cells were counted in each slide at 20x magnification. Normalization was performed at number of positive cells per mm^2 and means were estimated for statistical analysis.

4.6.Statistical analyses

All data was statistically analyzed and graphed in GraphPad Prism (version 9.3.1). For flow cytometry analysis, mixed-effect analysis with Tukey's post hoc test was performed. For histological and immunohistochemical analysis, paired *t*-test was used to compare treated skin with untreated skin within same genotype. In addition, two-way ANOVA test with Tukey's post hoc comparison was used to compare skin samples between genotypes. *P* values less than 0.05 were considered as significant.

References

1. Tensen CP, Quit KD, Vermeer MH. Genetic and epigenetic insights into cutaneous T-cell lymphoma. Blood. 2022;139(1):15-33. doi: 10.1182/blood.2019004256.
2. Bastidas Torres AN, Cats D, Mei H, Szuhai K, Willemze R, Vermeer MH, et al. Genomic analysis reveals recurrent deletion of JAK-STAT signaling inhibitors HNRNPK and SOCS1 in mycosis fungoides. Genes Chromosomes Cancer. 2018;57(12):653-64. doi: 10.1002/gcc.22679.
3. Park J, Daniels J, Wartewig T, Ringbloom KG, Martinez-Escala ME, Choi S, et al. Integrated genomic analyses of cutaneous T-cell lymphomas reveal the molecular bases for disease heterogeneity. Blood. 2021;138(14):1225-1236. doi: 10.1182/blood.2020009655.
4. Wang Z, Qiu H, He J, Liu L, Xue W, Fox A, et al. The emerging roles of hnRNPK. J Cell Physiol. 2020;235(3):1995-2008. doi: 10.1002/jcp.29186.
5. Mucha B, Qie S, Bajpai S, Tarallo V, Diehl JN, Tedeschi F, et al. Tumor suppressor mediated ubiquitylation of hnRNPK is a barrier to oncogenic translation. Nat Commun. 2022;13(1):6614. doi: 10.1038/s41467-022-34402-6.
6. Chen Y, Zeng Y, Xiao Z, Chen S, Li Y, Zou J, et al. Role of heterogeneous nuclear ribonucleoprotein K in tumor development. J Cell Biochem. 2019;120(9):14296-305. doi: 10.1002/jcb.28867.
7. Gallardo M, Lee HJ, Zhang X, Bueso-Ramos C, Pageon LR, McArthur M, et al. hnRNP K Is a Haploinsufficient Tumor Suppressor that Regulates Proliferation and Differentiation Programs in Hematologic Malignancies. Cancer Cell. 2015;28(4):486-99. doi: 10.1016/j.ccell.2015.09.001.
8. Inoue K, Fry EA. Haploinsufficient tumor suppressor. Adv Med Biol. 2017;118:83-122. PMID: 28680740.
9. Kwabi-Addo B, Giri D, Schmidt K, Podsypanina K, Parsons R, Greenberg N, et al. Haploinsufficiency of the Pten tumor suppressor gene promotes prostate cancer progression. PNAS. 2001;98(20):11563-11568. doi: 10.1073/pnas.201167798.
10. Davoli T, Xu AW, Mengwasser KE, Sack LM, Yoon JC, Park PJ, et al. Cumulative haploinsufficiency and triplosensitivity drive aneuploidy patterns and shape the cancer genome. Cell. 2013;155(4):948-962. doi: 10.1016/j.cell.2013.10.011.
11. Luo Y, Vermmer M, de Haan S, Kinderman P, de Gruijl FR, van Hall T, et al. Socs1-knockout in skin-resident CD4(+) T cells in a protracted contact-allergic reaction results in an autonomous skin inflammation with features of early-stage mycosis fungoides. Biochem Biophys Rep. 2023;35:101535. doi: 10.1016/j.bbrep.2023.101535.
12. Popović B, Nicolet BP, Guislain A, Engels S, Jurgens AP, Paravinja N, et al. Time-dependent regulation of cytokine production by RNA binding proteins defines T cell effector function. Cell Rep. 2023;42(5):112419. doi: 10.1016/j.celrep.2023.112419.
13. Kerstin Rahn, Isabel Naarmann-de Vrie, Yvonne Sackmann, Felicitas Klein, Antje Ostareck-Lederer, Dirk Ostareck, et al. Role of hnRNP K and Interacting mRNAs in Pathogenesis of AML with 9q Deletion. Blood. 2018;132(Supplement 1):1531. doi: 10.1182/blood-2018-99-114699
14. Li M, Yang X, Zhang G, Wang L, Zhu Z, Zhang W, et al. Heterogeneous nuclear ribonucleoprotein K promotes the progression of lung cancer by inhibiting the p53-dependent signaling pathway. Thorac Cancer. 2022;13(9):1311-1321. doi: 10.1111/1759-7714.14387.

15. Carpenter B, McKay M, Dundas SR, Lawrie LC, Telfer C, Murray GI. Heterogeneous nuclear ribonucleoprotein K is over expressed, aberrantly localised and is associated with poor prognosis in colorectal cancer. Br J Cancer. 2006;95(7):921-7. doi: 10.1038/sj.bjc.6603349.

16. Ciarlo M, Benelli R, Barbieri O, Minghelli S, Barboro P, Balbi C, et al. Regulation of neuroendocrine differentiation by AKT/hnRNPK/AR/b-catenin signaling in prostate cancer cells. Int J Cancer. 2011;131(3):582-90. doi: 10.1002/ijc.26402.

17. Wen F, Shen A, Shanas R, Bhattacharyya A, Lian F, Hostetter G, et al. Higher Expression of the Heterogeneous Nuclear Ribonucleoprotein K in Melanoma. Ann Surg Oncol. 2010;17(10):2619-27. doi: 10.1245/s10434-010-1121-1.

18. Iwabuchi E, Miki Y, Suzuki T, Hirakawa H, Ishida T, Sasano H. Heterogeneous Nuclear Ribonucleoprotein K Is Involved in the Estrogen-Signaling Pathway in Breast Cancer. Int J Mol Sci. 2021;22(5).2581. doi: 10.3390/ijms22052581.

19. Zhou W, Jie Q, Pan T, Shi J, Jiang T, Zhang Y, et al. Single-cell RNA binding protein regulatory network analyses reveal oncogenic HNRNPK-MYC signalling pathway in cancer. Commun Biol. 2023;6(1):82. doi: 10.1038/s42003-023-04457-2.

20. Zohdy M, Abd El Hafez A, Abd Allah MYY, Bessar H, Refat S. Ki67 and CD31 Differential Expression in Cutaneous T-Cell Lymphoma and Its Mimickers: Association with Clinicopathological Criteria and Disease Advancement. Clin Cosmet Investig Dermatol. 2020;13:431-42. doi:10.2147/CCID.S256269

21. Shen X, Wang B, Li K, Wang L, Zhao X, Xue F, et al. MicroRNA Signatures in Diagnosis and Prognosis of Cutaneous T-Cell Lymphoma. J Invest Dermatol. 2018;138(9):2024-32. doi: 10.1016/j.jid.2018.03.1500.

22. Chang JW, Koike T, Iwashima M. hnRNP-K is a nuclear target of TCR-activated ERK and required for T-cell late activation. Int Immunol. 2009;21(12):1351-1361. doi: 10.1093/intimm/dxp106.

23. Sengupta S, West K, Sanghvi S, Laliotis G, Agosto LM, Lynch KW, et al. PRMT5 Promotes Symmetric Dimethylation of RNA Processing Proteins and Modulates Activated T Cell Alternative Splicing and Ca(2+)/NFAT Signaling. Immunohorizons. 2021;5(10):884-97. doi: 10.4049/immunohorizons.2100076.

24. Sommer VH, Clemmensen OJ, Nielsen O, Wasik M, Lovato P, Brender C, et al. In vivo activation of STAT3 in cutaneous T-cell lymphoma. Evidence for an antiapoptotic function of STAT3. Leukemia. 2004;18(7):1288-95. doi: 10.1038/sj.leu.2403385.

25 Yu H, Kortylewski M, Pardoll D. Crosstalk between cancer and immune cells: role of STAT3 in the tumour microenvironment. Nat Rev Immunol. 2007;7(1):41-51. doi: 10.1038/nri1995.

26. Gluud M, Pallesen EMH, Buus TB, Gjerdrum LMR, Lindahl LM, Kamstrup MR, et al. Malignant T cells induce skin barrier defects through cytokine-mediated JAK/STAT signaling in cutaneous T-cell lymphoma. Blood. 2023;141(2):180-93. doi: 10.1182/blood.2022016690.

27. Olszewska B, Zawrocki A, Lakomy J, Karczewska J, Glen J, Zablotna M, et al. Mapping signal transducer and activator of transcription (STAT) activity in different stages of mycosis fungoides and Sezary syndrome. Int J Dermatol. 2020;59(9):1106-12. doi: 10.1111/ijd.15036.

28. Fanok MH, Sun A, Fogli LK, Narendran V, Eckstein M, Kannan K, et al. Role of Dysregulated Cytokine Signaling and Bacterial Triggers in the Pathogenesis of Cutaneous T-Cell Lymphoma. J Invest

Dermatol. 2018;138(5):1116-25. doi: 10.1016/j.jid.2017.10.028.
29. Huang H, Han Y, Yang X, Li M, Zhu R, Hu J, et al. HNRNPK inhibits gastric cancer cell proliferation through p53/ p21/CCND1 pathway. Oncotarget. 2017;8(61):103364-103374. doi: 10.18632/oncotarget.
30. Sudhakaran M, Doseff A. Role of Heterogeneous Nuclear Ribonucleoproteins in the Cancer-Immune Landscape. Int J Mol Sci. 2023;24(6):5086. doi: 10.3390/ijms24065086.
31. Lu ZY, Chen P, Xu QY, Li B, Jiang SD, Jiang LS, et al. Constitutive and conditional gene knockout mice for the study of intervertebral disc degeneration: Current status, decision considerations, and future possibilities. JOR Spine. 2023;6(1): e1242. doi: 10.1002/jsp2.1242.
32. Lampreht Tratar U, Horvat S, Cemazar M. Transgenic Mouse Models in Cancer Research. Front Oncol. 2018;8:268. doi: 10.3389/fonc.2018.00268.
33. Luo Y, Vermeer MH, de Gruijl FR, Zoutman WH, Sluijter M, van Hall T, et al. In vivo modelling of cutaneous T-cell lymphoma: The role of SOCS1. Front Oncol. 2022;12:1031052. doi: 10.3389/fonc.2022.1031052.

Supplementary Information

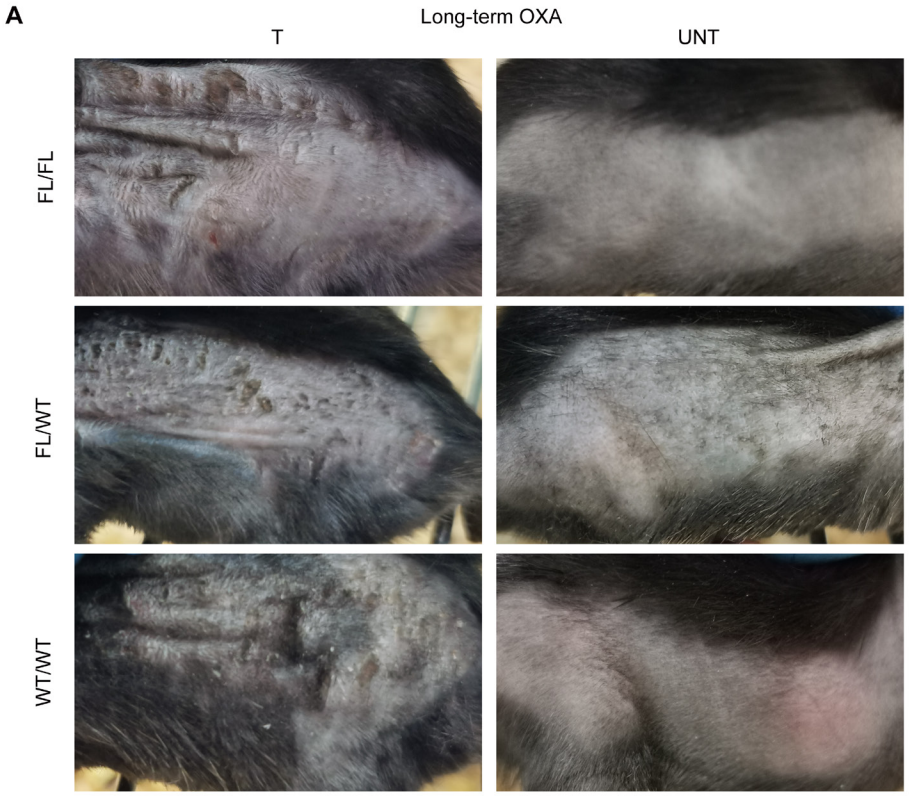

Supplementary Figure 1. Macroscopic analysis of treated and untreated skin from *Hnrnpk fl/fl Cd4CreER^{T2}+/-*, *Hnrnpk fl/wt Cd4CreER^{T2}+/-* and *Hnrnpk wt/wt Cd4CreER^{T2}+/-* mice shows presence of inflammation symptoms in treated skins in the long-term group.

Representative clinical photos of treated and untreated skin images of *Hnrnpk fl/fl Cd4CreER^{T2}+/-*, *Hnrnpk fl/wt Cd4CreER^{T2}+/-* and *Hnrnpk wt/wt Cd4CreER^{T2}+/-* mice of the long-term treatment group.

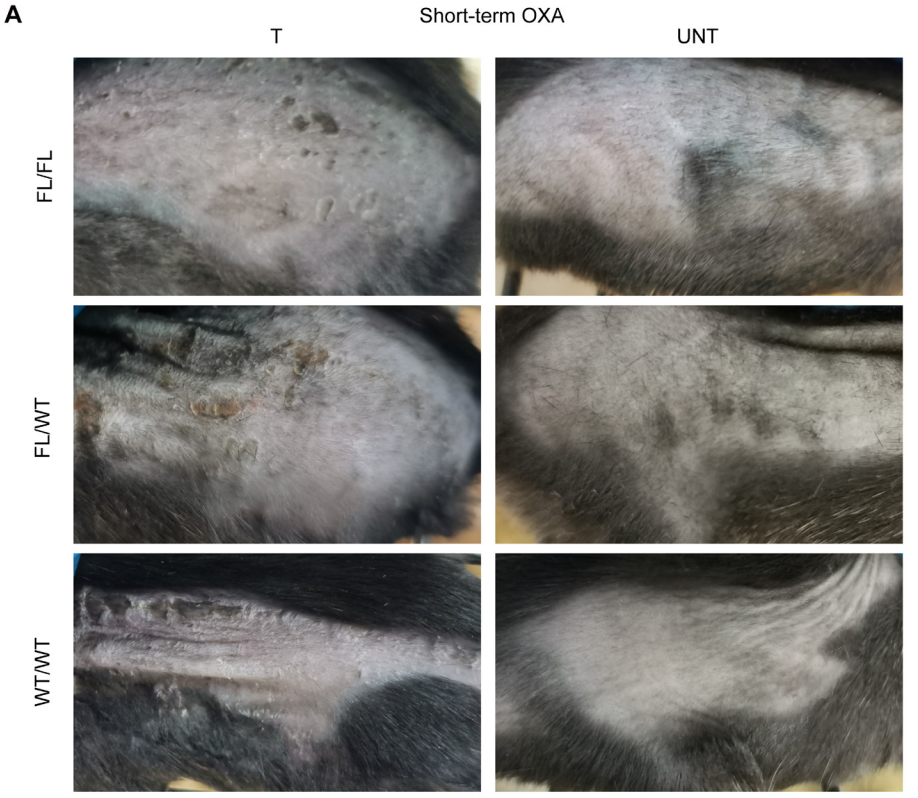

Supplementary Figure 2. Macroscopic analysis of treated and untreated skin from *Hnrnpk fl/fl Cd4CreER^{T2}+/-*, *Hnrnpk fl/wt Cd4CreER^{T2}+/-* and *Hnrnpk wt/wt Cd4CreER^{T2}+/-* mice shows presence of inflammation symptoms in treated skins in the short-term treatment group.

Representative clinical photos of treated and untreated skin images of *Hnrnpk fl/fl Cd4CreER^{T2}+/-*, *Hnrnpk fl/wt Cd4CreER^{T2}+/-* and *Hnrnpk wt/wt Cd4CreER^{T2}+/-* mice of the short-term treatment group.

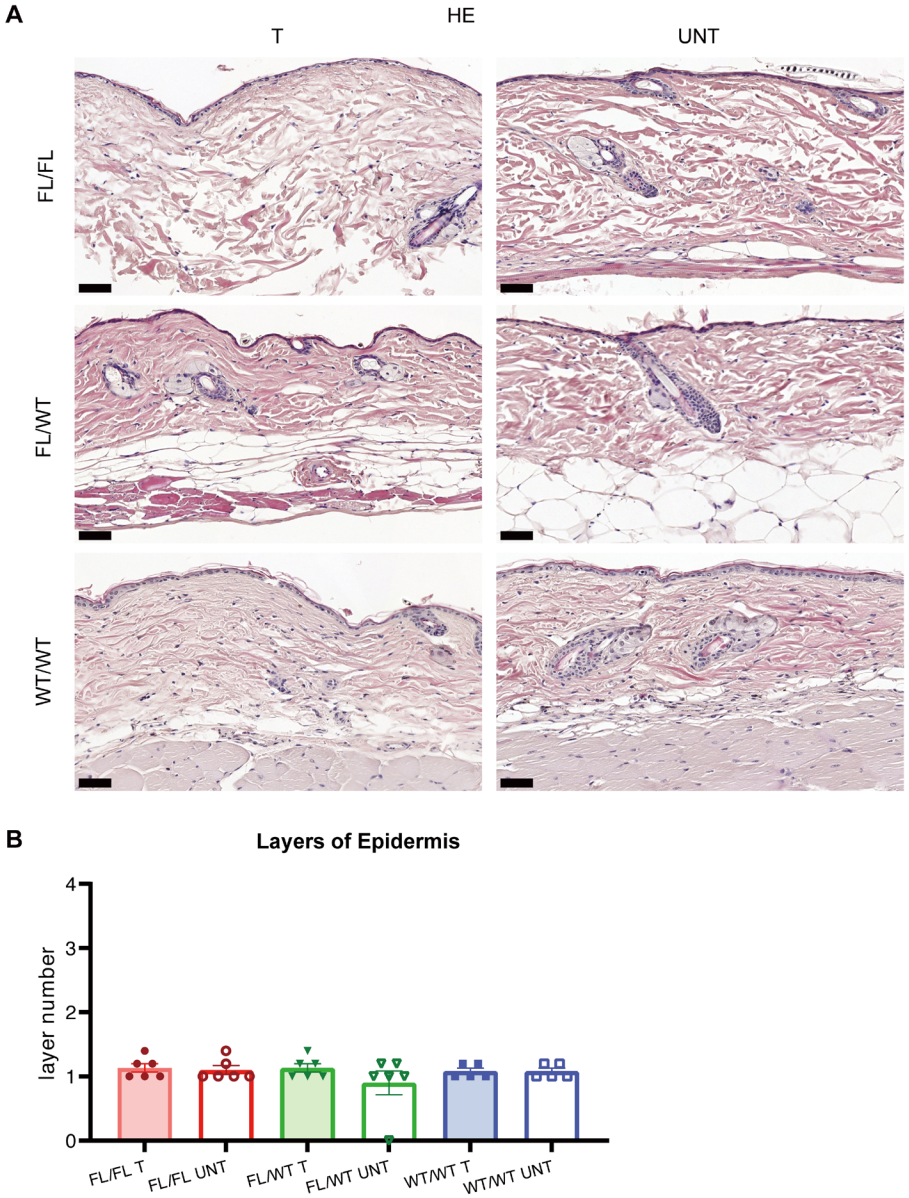

Supplementary Figure 3. Histological analysis of treated and untreated skin from *Hnrnpk fl/fl Cd4CreER^{T2}+/-*, *Hnrnpk fl/wt Cd4CreER^{T2}+/-* and *Hnrnpk wt/wt Cd4CreER^{T2}+/-* mice of the short-term treatment group demonstrates no changes in number of epidermal layers. (A) Treated and untreated skin sections of *Hnrnpk fl/fl Cd4CreER^{T2}+/-*, *Hnrnpk fl/wt Cd4CreER^{T2}+/-* and *Hnrnpk wt/wt Cd4CreER^{T2}+/-* mice stained with the HE staining. Magnification is 20x and scale bar is 50 µm. B) Quantification of the number of epidermal layers of treated and untreated skin from *Hnrnpk fl/*

fl Cd4CreER^{T2}+/-, *Hnrnpk fl/wt Cd4CreER*^{T2}+/- and *Hnrnpk wt/wt Cd4CreER*^{T2}+/- mice. A paired t-test and two-way ANOVA with a Tukey's post hoc test were used for statistical analysis and error bars representing standard errors of the mean (SEM). n is 5 or 6 per genotype.

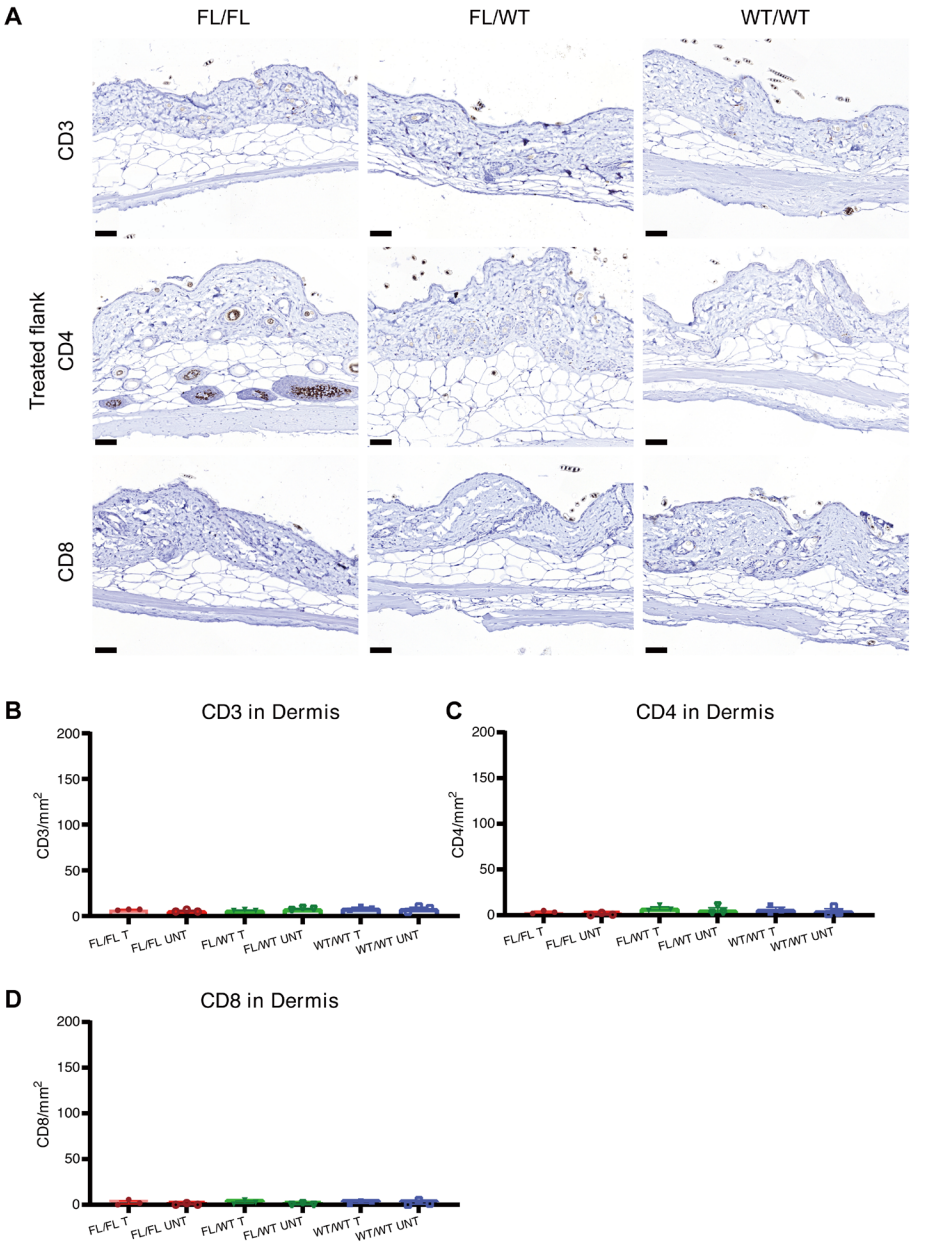

Supplementary Figure 4. Histological analysis of treated skin from *Hnrnpk fl/fl Cd4CreER*^{T2}+/-, *Hnrnpk*

fl/wt Cd4CreER^{T2}+/- and *Hnrnpk wt/wt Cd4CreER*^{T2}+/- mice of the short-term treatment group demonstrates no differences in number of CD3, CD4 and CD8 cells in the dermis. (A) Treated skin sections of *Hnrnpk fl/fl Cd4CreER*^{T2}+/-, *Hnrnpk fl/wt Cd4CreER*^{T2}+/- and *Hnrnpk wt/wt Cd4CreER*^{T2}+/- mice stained with CD3, CD4 and CD8 IHC staining. Magnification is 20x and scale bar is 50 µm. Black arrows indicate stained cells. B, C, D) Quantification of the positive stained CD3 (B), CD4 (C) and CD8 (D) cells in the dermis of treated and untreated skin from *Hnrnpk fl/fl Cd4CreER*^{T2}+/-, *Hnrnpk fl/wt Cd4CreER*^{T2}+/- and *Hnrnpk wt/wt Cd4CreER*^{T2}+/- mice. A paired t-test and two-way ANOVA with a Tukey's post hoc test were used for statistical analysis. Error bars represent SEM and n is 3 per genotype.

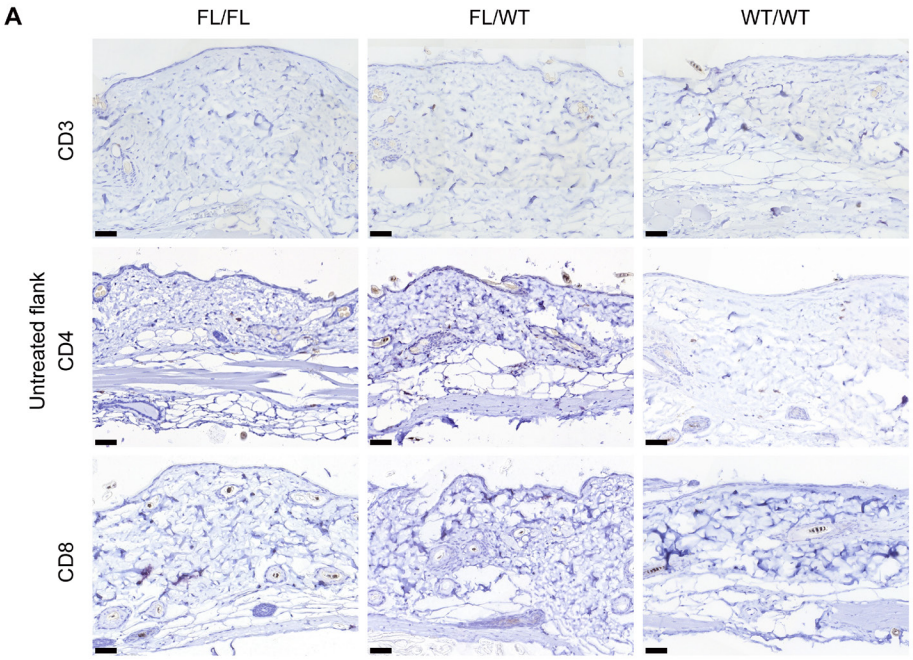

Supplementary Figure 5. Histological analysis of untreated skin from *Hnrnpk fl/fl Cd4CreER*^{T2}+/-, *Hnrnpk fl/wt Cd4CreER*^{T2}+/- and *Hnrnpk wt/wt Cd4CreER*^{T2}+/- mice of the long-term treatment group reveals unchanged number of CD3, CD4 and CD8 cells in the dermis. Untreated skin sections of *Hnrnpk fl/fl Cd4CreER*^{T2}+/-, *Hnrnpk fl/wt Cd4CreER*^{T2}+/- and *Hnrnpk wt/wt Cd4CreER*^{T2}+/- mice stained with CD3, CD4 and CD8. Magnification is 20x and scale bar is 50 µm. Black arrows indicate positive stained cells. n is 5 or 6 per genotype.

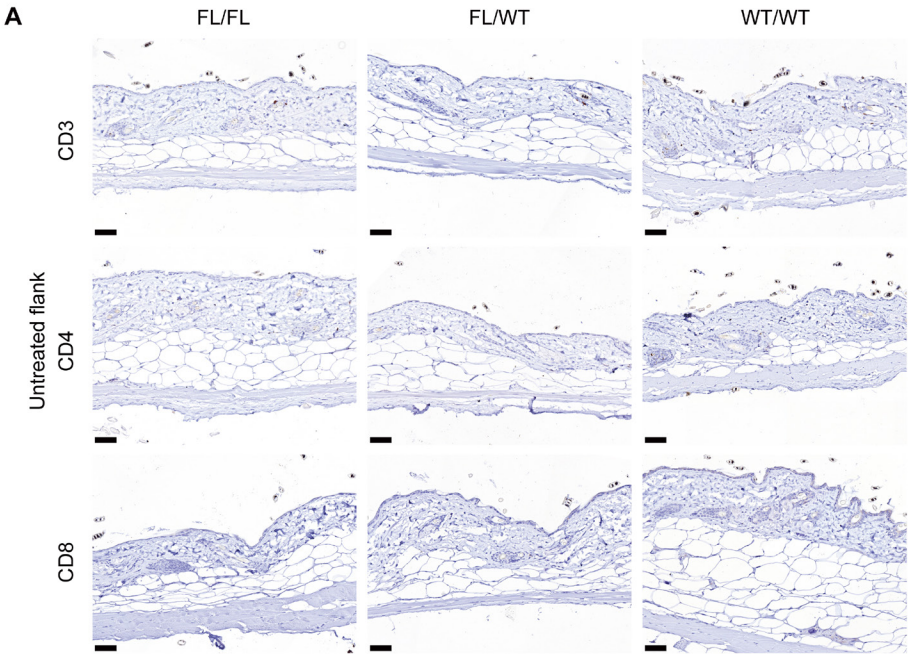

Supplementary Figure 6. Histological analysis of untreated skin from *Hnrnpk fl/fl Cd4CreER^{T2}+/-*, *Hnrnpk fl/wt Cd4CreER^{T2}+/-* and *Hnrnpk wt/wt Cd4CreER^{T2}+/-* mice of the short-term treatment group demonstrates no differences in number of CD3, CD4 and CD8 cells in the dermis. Untreated skin sections of *Hnrnpk fl/fl Cd4CreER^{T2}+/-*, *Hnrnpk fl/wt Cd4CreER^{T2}+/-* and *Hnrnpk wt/wt Cd4CreER^{T2}+/-* mice stained with CD3, CD4 and CD8. Magnification is 20x and scale bar is 50 µm. Black arrows indicate positive stained cells. n is 3 per genotype.

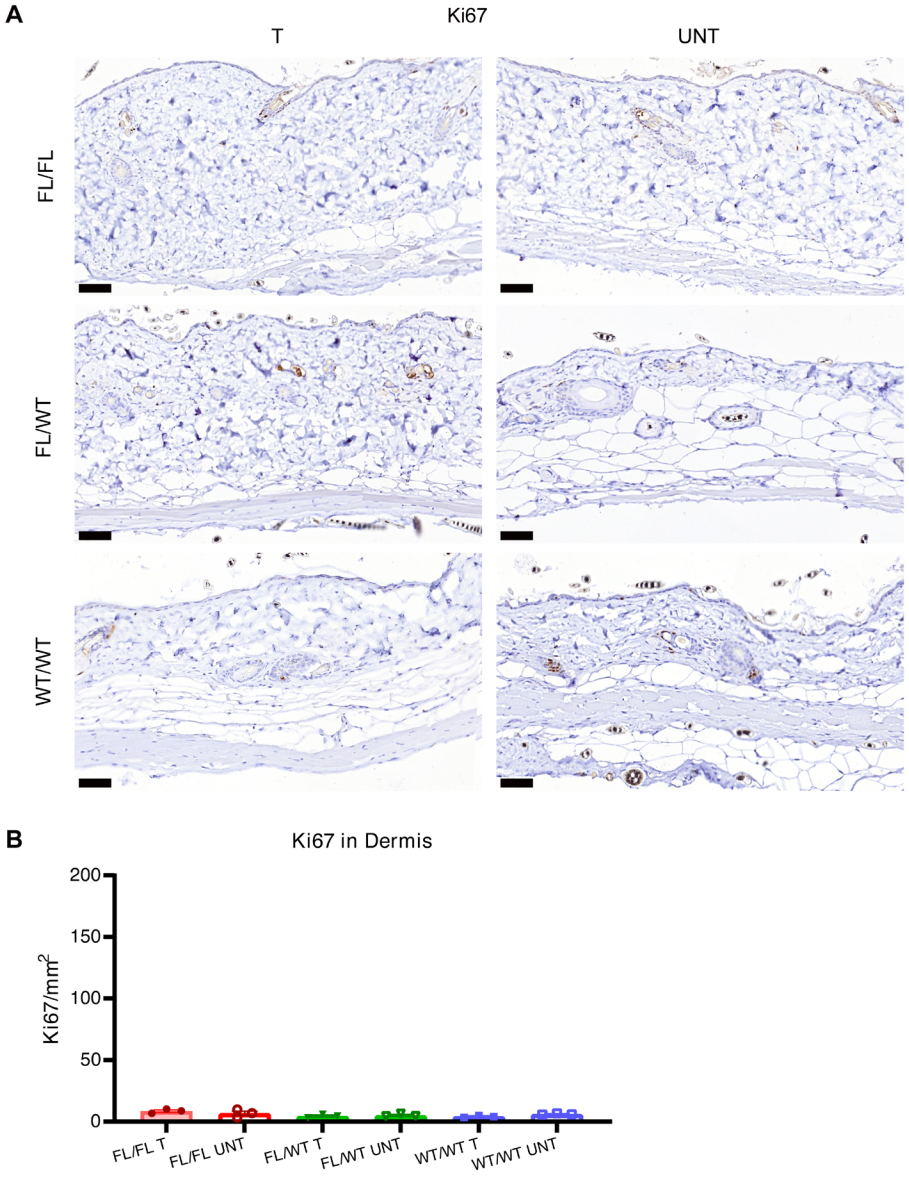

Supplementary Figure 7. Histological analysis of treated and untreated skins from *Hnrnpk fl/fl Cd4CreER^{T2}+/-*, *Hnrnpk fl/wt Cd4CreER^{T2}+/-* and *Hnrnpk wt/wt Cd4CreER^{T2}+/-* mice of the short-term treatment group shows no changes in number of Ki-67 positive cells in the dermis.

A) Treated and untreated skin sections of *Hnrnpk fl/fl Cd4CreER^{T2}+/-*, *Hnrnpk fl/wt Cd4CreER^{T2}+/-* and *Hnrnpk wt/wt Cd4CreER^{T2}+/-* mice stained with Ki-67. Magnification is 20x and scale bar is 50 µm. Black arrows indicate stained cells. B) Quantification of the positive Ki-67 cells in the dermis of

treated and untreated skin from *Hnrnpk fl/fl Cd4CreER^{T2}+/-*, *Hnrnpk fl/wt Cd4CreER^{T2}+/-* and *Hnrnpk wt/wt Cd4CreER^{T2}+/-* mice. Paired t-test and two-way ANOVA with a Tukey's post hoc test were used for statistical analysis. Error bars represent SEM and n is 5 or 6 per genotype.

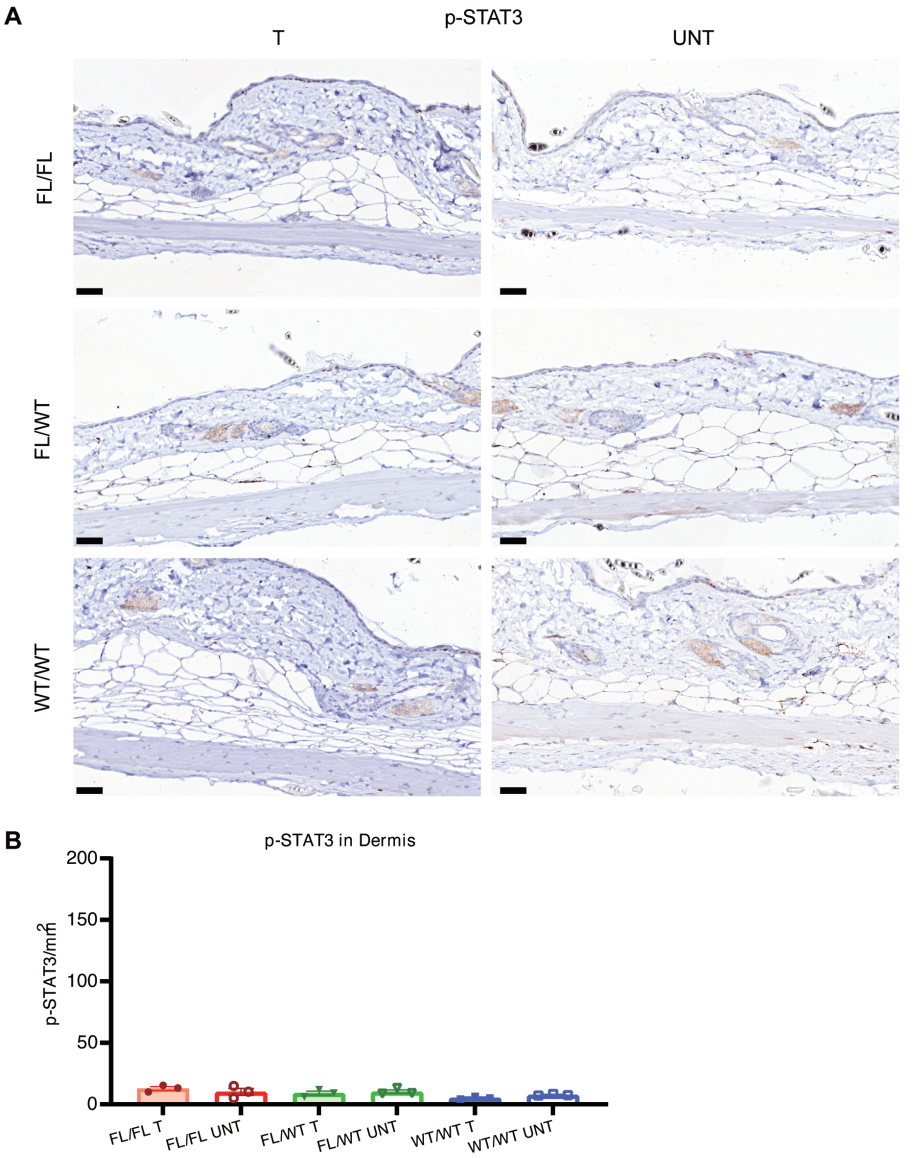

Supplementary Figure 8. Histological analysis of treated and untreated skins from *Hnrnpk fl/fl Cd4CreER^{T2}+/-*, *Hnrnpk fl/wt Cd4CreER^{T2}+/-* and *Hnrnpk wt/wt Cd4CreER^{T2}+/-* mice of the short-term treatment group shows no changes in number of p-STAT3 positive cells in the dermis.

A) Treated and untreated skin sections of *Hnrnpk fl/fl Cd4CreER^{T2}+/-*, *Hnrnpk fl/wt Cd4CreER^{T2}+/-* and *Hnrnpk wt/wt Cd4CreER^{T2}+/-* mice stained with p-STAT3. Magnification is 20x and scale bar is 50 µm. Black arrows indicate stained cells. B) Quantification of the positive stained p-STAT3 cells in the dermis of treated and untreated skin from *Hnrnpk fl/fl Cd4CreER^{T2}+/-*, *Hnrnpk fl/wt Cd4CreER^{T2}+/-* and *Hnrnpk wt/wt Cd4CreER^{T2}+/-* mice. Paired t-test and two-way ANOVA with a Tukey's post hoc test were used for statistical analysis. Error bars represent SEM and n is 5 or 6 per genotype.